



**Environmental  
Science**  
Water Research & Technology

**Photochemical Conversion of Nitrate to Ammonium Ion by a  
Newly Developed Photo-Reductive Titanium Dioxide  
Catalyst: Implications on Nitrogen Recovery**

Journal:	<i>Environmental Science: Water Research &amp; Technology</i>
Manuscript ID	EW-COM-07-2023-000523.R1
Article Type:	Communication

**SCHOLARONE™**  
Manuscripts

## **Water Impact Research Statement**

Nitrate contamination in natural groundwaters is an important environmental issue, while ammonia is preferable nitrogen product for resource recovery. This study developed a photocatalytic titanium dioxide nanoparticle and successfully demonstrated the conversion of ammonia from nitrate contaminated waters to valuable ammonia end product with a higher yield via photocatalytic nitrate reduction.

**Photochemical Conversion of Nitrate to Ammonium Ion by a Newly Developed Photo-Reductive Titanium Dioxide Catalyst: Implications on Nitrogen Recovery**

Andrew Sanchez<sup>1</sup>, Zuyang Ye<sup>2</sup>, Yadong Yin<sup>2</sup> and Haizhou Liu<sup>1,\*</sup>

<sup>1</sup> Department of Chemical and Environmental Engineering, University of California at Riverside,  
Riverside, CA 92521 USA

<sup>2</sup> Department of Chemistry, University of California at Riverside, Riverside CA 92521 USA

\* Corresponding author, email: haizhou@engr.ucr.edu

Phone: (951) 827-2076, fax (951) 827-5696.

Submitted to *Environmental Science: Water Research & Technology*

**Abstract**

Global nitrate contamination in source water poses a threat to both natural ecosystem and public health. This study developed a photo-reductive titanium dioxide ( $\text{TiO}_2$ ) nanoparticle with surface-grafted diethylene glycol (DEG) ligands to photochemically degrade nitrate under medium-pressure UV irradiation and convert it to the desirable end product ammonium. The new catalyst was synthesized via a sustainable and non-harsh synthesis approach. Nitrate was efficiently removed at a rate 6 times faster than a standard commercial photo-oxidative photocatalyst, and the formation of the intermediate byproduct nitrite was minimized. The ammonium selectivity highly depended on the synthesis temperature of the catalyst. The synthesis temperature was examined from  $190^\circ\text{C}$  to  $230^\circ\text{C}$  and revealed that the higher temperature of  $230^\circ\text{C}$  enhanced nitrate reduction and ammonia production, likely by means of increasing the crystallinity of the catalyst. Ammonium can be harvested at approximately 70% of the initial nitrate concentration. This study highlights the efficacy of photo-reductive  $\text{TiO}_2$  to remove nitrate while simultaneously producing ammonium ion, providing a promising technology for denitrification and nitrogen resource recovery.

**Key words:** Nitrate Reduction, Titanium Dioxide, Ammonium Generation, Photocatalysis

## 1. Introduction

The application of agricultural fertilizer and impacts from anthropogenic activities including the combustion of fossil fuels and factory emissions result in nitrate ( $\text{NO}_3^-$ ) contamination in surface and groundwaters, which poses a global threat to the environment and public health.<sup>1-3</sup> Nitrate enrichment in the ecosystem leads to eutrophication and toxic algal blooms.<sup>4</sup> Human exposure to nitrate can lead to methemoglobinemia and cancer.<sup>5</sup> The maximum contaminant level (MCL) for nitrate in drinking water is 10 mg-N/L.<sup>6</sup> Furthermore, as the global demand for water and nitrogen-based fertilizer increases, risks of severe nitrate contamination will rise.<sup>7</sup>

Traditional water treatment to remove nitrate include ion exchange, biological denitrification and membrane separation,<sup>8-12</sup> but each technology has its own limitations. For example, ion exchange generates large volumes of waste brine that requires costly disposal.<sup>13,14</sup> Biological denitrification requires the addition of organic substrates as electron donors, requires a long operating time, and generates toxic waste sludge that needs further treatment.<sup>12,14,15</sup> Furthermore, it is preferable to reductively convert nitrate to ammonium ion ( $\text{NH}_4^+$ ) as the end product, because  $\text{NH}_4^+$  is a desirable form of nitrogen species for nutrient recovery with a high global demand.<sup>16-18</sup>  $\text{NH}_4^+$  is a multifunctional compound useful as a refrigerant, fertilizer, energy carrier, and chemical precursor.<sup>17,19</sup> However, traditional treatment technologies are not capable of selectively producing ammonium ion from nitrate. For example, biological denitrification produces nitrogen gas as the end product while ion exchange and membrane separation only partition nitrate from the feedwater to a second medium without changing its chemical form. In addition, although electrochemical denitrification can reduce nitrate to ammonium and

hydroxylamine, it requires the use of costly and scarce noble metals as electrodes, and the corrosion of transition metal-electrodes introduces additional contaminants.<sup>14,19–21</sup>

Photocatalytic nitrate conversion provides a promising alternative to effectively reduce nitrate to ammonium ion. Previous studies demonstrated the application of titanium dioxide (TiO<sub>2</sub>) nanocrystals for environmental mitigation due to their high stability and low toxicity.<sup>22,23</sup> When TiO<sub>2</sub> is irradiated by ultraviolet photons with energy equal to or higher than its band gap ( $E = 3.0\text{--}3.2\text{ eV}$ ), the electrons in its valence band are excited to the conduction band and become photogenerated electrons, whereas photogenerated holes are left in the valence band and react with water molecules to generate highly oxidative hydroxyl radicals.<sup>24</sup> Meanwhile, the electron-hole recombination makes photogenerated electrons unavailable. Therefore, traditional TiO<sub>2</sub> is highly oxidative in nature.<sup>25–27</sup> For example, conventional photo-oxidative TiO<sub>2</sub> photocatalysts such as Degussa P25 are widely available and have been applied for oxidative water treatment in organic carbon degradation.

To develop photo-reductive TiO<sub>2</sub>, the photogenerated electrons need to be separated from the electron-hole pairs to avoid recombination. Because the electrons recombine with the generated holes on the surface of TiO<sub>2</sub> within nanoseconds, it typically requires the addition of external hole scavengers to serve as electron donors to trap holes, thus leaving electrons available for nitrate reduction.<sup>13</sup> External organic hole scavengers including organic compounds (*e.g.*, methanol and formic acid) and inorganic compounds (*e.g.*, S<sup>2-</sup> and I<sup>-</sup>) have been investigated.<sup>28–30</sup> However, because of the low scavenging efficiency, the dosing of scavengers requires a large quantity and often results in a chemical residual and secondary pollution of the process.<sup>7</sup>

Therefore, it is vitally important to design a new  $\text{TiO}_2$  catalyst with internal hole-scavenging capabilities to facilitate a reductive conversion of nitrate to ammonium ion. Recently, diethylene glycol (DEG) was discovered as a promising doping chemical reagent to synthesize DEG-doped  $\text{TiO}_2$  with a strong capacity to release photogenerated electrons, therefore producing photo-reductive  $\text{TiO}_2$  that converted hexavalent chromium to trivalent chromium.<sup>31</sup> Chelating nanoparticles with polyols serve to prevent charge-carrier recombination, allowing for the availability of electrons for further reduction processes. DEG, when used as a sacrificial electron donor (SED), markedly amplifies the photocatalytic reduction capabilities of  $\text{TiO}_2$  nanocrystals. DEG was selected because poly-hydroxyl molecules are shown to induce filled gaps and therefore possess more efficient hole scavenging capabilities than by mono-hydroxyl molecules.<sup>30,31</sup>

Recently, graphitic carbon nitride ( $\text{g-C}_3\text{N}_4$ ) has effective solar energy conversion applications including photocatalytic reduction of nitrate. Furthermore, the usage of solar energy compared to UV treatment offers an alternative to treatment and reduction of nitrate. However, it also suffers limitations from electron-hole recombination. This is mitigated by hybrid structures such as loading silver loading, which also demonstrates the promising denitrification strategy to reduce aqueous nitrate to nitrogen gas and ammonium.<sup>32,33</sup> However, the conversion yield of nitrate to ammonium is very low (<25%) and a majority of nitrate is converted to nitrite (>80%), which is even more toxic than nitrate. Other technological options, such as Metal-Organic-Frameworks (MOFS) and metal-sulfide compounds provide alternatives to nitrate reduction. Electrocatalytic nitrogen reduction (NRR), although in nascent stages, is argued to be promising due to the high

efficiency.<sup>34</sup> However, the use of such technologies includes the use of potent residual metal toxins and aqueous organics.<sup>35,36</sup> Thus, a non-harsh sustainable approach to reductive treatment is needed.

Taking advantage of its photo-reductive properties, the photocatalytic reduction of nitrate in the presence of DEG-doped TiO<sub>2</sub> can be performed. The challenge, however, is that toxic byproducts such as nitrite can be produced. Therefore, a clear understanding of nitrogen transformation selectivity is desired to mitigate the nitrite production and promote the formation of useful end products such as ammonium ion. Accordingly, the objective of this investigation is to synthesize a TiO<sub>2</sub> photocatalyst by surface grafting with DEG for enhanced nitrate reduction and selective ammonium production while minimizing nitrite formation. Furthermore, to optimize the performance of the system, the synthesis temperature of TiO<sub>2</sub> was optimized to increase the selectivity of ammonium as the final product. A detailed investigation of this nitrogen speciation was conducted in order to optimize the selectivity of ammonium. Accordingly, this technology was applied to simulate nitrate reduction in the context of synthetic groundwater.

## **2. Materials and Methods**

### **2.1 Synthesis of photo-reductive TiO<sub>2</sub> catalysts**

All chemicals were analytical grade. All stock solutions were prepared fresh daily using deionized water (resistivity  $\geq 18.2$  M $\Omega$ /cm). Photo-reductive TiO<sub>2</sub> nanocrystals were synthesized by injecting 0.2 mL of TiCl<sub>4</sub> into 20 mL of pure DEG with 5 mL of H<sub>2</sub>O. The mixture was



heated for hydrolysis at a targeted temperature between 190°C and 230°C to hydrolyze  $\text{TiCl}_4$  and generate  $\text{TiO}_2$  nanocrystals, which were then precipitated out by adding acetone and centrifuged at 8,000 rpm for 7 minutes. The hydrolysis time was optimized to 3 hours to chemically bond the DEG molecules to the surface of the  $\text{TiO}_2$  crystal.<sup>31</sup> The final product of photo-reductive  $\text{TiO}_2$  was washed twice with acetone to remove any residuals and then redispersed in 10 mL of  $\text{H}_2\text{O}$ .

## 2.2 Photochemical denitrification experiments

Bench-scale photochemical denitrification experiments were performed in 8 mL quartz tubes placed in a carousel reactor (Ace Glass, Inc). The synthesized  $\text{TiO}_2$  suspension was sonicated for 15-20 minutes. The reaction solution was prepared by mixing 1.6 mM nitrate with 50 mg/L  $\text{TiO}_2$  and controlled at pH of 7 by using 20 mM phosphate buffer. Following that, the reaction solution was transferred to sacrificial quartz tubes and rotated around a 450-W medium pressure ultra-violet lamp with a light intensity of 42 mW/cm<sup>2</sup> emitting polychromatic light ranging from 200 to 850 nm. The spectral irradiance of this lamp along with the UV-vis spectra of synthetic and industrial  $\text{TiO}_2$  is provided in Figure S1 of Supporting Information (SI). Results indicate that photo-oxidative  $\text{TiO}_2$  absorbs a smaller fraction of light with respect to photo-reductive  $\text{TiO}_2$ . To evaluate the photo-reductive  $\text{TiO}_2$  performance, three additional control experiments were conducted, including a UV control in the absence of UV light to evaluate adsorption effects of the synthesized  $\text{TiO}_2$  on nitrate removal, a catalyst control in the absence of  $\text{TiO}_2$  to evaluate nitrate direct photolysis effects, and a photo-oxidative  $\text{TiO}_2$  control in which photo-oxidative P25  $\text{TiO}_2$  catalyst, and externally added DEG, was used to reduce nitrate. Commercialized Aeroxide P25  $\text{TiO}_2$  was purchased from Acros Organics. At each pre-determined sampling time intervals,

3 sacrificial quartz tubes were withdrawn from the carousel reactor. The suspension in each tube was filtered through a 0.22- $\mu\text{m}$  filter and stored for subsequent chemical analysis. All experiments were conducted at 25°C in triplicates. Furthermore, to test the feasibility of this photocatalyst, synthetic groundwater (chemical composition shown in Table S1) was prepared and tested in presence of synthesized  $\text{TiO}_2$ .

### 2.3 Analytic methods

The morphology of the synthesized photo-reductive  $\text{TiO}_2$  catalysts was characterized using a Talos 120C transmission electron microscope (TEM) operating at 120 kV. The Fourier transform infrared spectroscopy (FTIR) spectra of the catalyst were acquired on a Nicolet 6700 FTIR spectrometer to identify chemical bonds in the catalyst and to confirm the existence of surface-bonded DEG. Thermogravimetric analysis (TGA) was performed on the Seiko TA Instruments Thermogravimetric Analyzer under air atmosphere used to characterize the DEG content of the nanoparticles. 1-mL of the freshly prepared  $\text{TiO}_2$  aqueous suspension was digested in 2% HF and measured via Inductively Coupled Plasma Mass Spectrometry (ICP-MS) and analyzed for Ti content in the synthesized  $\text{TiO}_2$ , which were used to normalize the catalyst dosage for experiments. For filtered samples taken at different reaction times from the photochemical experiments, the concentrations of nitrate and nitrite were measured using the Standard Method (4500- $\text{NO}_2^-$ ) by a spectrophotometer at 410 and 543 nm, respectively.<sup>37</sup> The ammonium concentration was measured at 640 nm using the phenate method (4500- $\text{NH}_3\text{ F}$ ) and was detailed in Supporting Information (Text S1).<sup>37</sup> Total dissolved nitrogen were measured using a Total Organic Carbon (TOC) analyzer with a total nitrogen module (Shimadzu TOC-VSH).

### 3. Results and Discussion

#### 3.1 Characterization of TiO<sub>2</sub> Nanoparticles

The synthesized TiO<sub>2</sub> nanocrystals were 5-10 nm in size with irregular shapes, as indicated by the TEM image (Figure 1A). Various heating times were also conducted to compare the morphology (Figure S3). As the heating time increased, the morphology gradually transformed into a spindle shape, indicating an increase in the crystallinity of the TiO<sub>2</sub> nanocrystals. The presence of surface bonded DEG on TiO<sub>2</sub> was confirmed by FTIR. The absorption peaks of DEG molecules at 892, 1050, 1125 and 1234 cm<sup>-1</sup> correspond to the -OC<sub>2</sub>H<sub>4</sub> stretching, C-O stretching, C-C-O stretching and C-O-C stretching modes, respectively (Figure 1B). The absorption peaks at 1353 and 1454 cm<sup>-1</sup> correspond to the vibration of CH<sub>2</sub> in DEG. The major FTIR peaks of TiO<sub>2</sub> matched well with those in pure DEG solution, strongly suggesting the bonding of DEG on the TiO<sub>2</sub> surface. Importantly, the peak at 1050 cm<sup>-1</sup> in pure DEG shifted to 1085 cm<sup>-1</sup> in the spectrum of TiO<sub>2</sub> sample, which is strong evidence for the formation of C-O-Ti bond.<sup>23,38</sup> FTIR data confirmed the surface of TiO<sub>2</sub> nanocrystals is bonded with DEG. The molar ratio of TiO<sub>2</sub>-to-DEG on the surface of TiO<sub>2</sub> was 4.7, based on Ti content measured by ICP-MS and DEG concentration measured by TGA. The XRD was measured on a PANanalytical Empyrean Series 2 X-ray diffractometer with a copper target ( $\lambda=1.54 \text{ \AA}$ ). The XRD peaks showed that TiO<sub>2</sub> existed anatase-rutile mixed phases with low crystallinity (Figure 1C).

### 3.2 Photocatalytic reduction of nitrate in the presence of TiO<sub>2</sub>

Photochemical experiments revealed the efficacy of nitrate reduction in the presence of DEG-doped TiO<sub>2</sub> nanoparticles synthesized at 230°C (Figure 2). The synthetic photo-reductive TiO<sub>2</sub> exhibited a much greater efficiency and faster nitrate reduction kinetics than traditional photo-oxidative TiO<sub>2</sub>. For example, the photo-oxidative TiO<sub>2</sub>, which contains P25 and DEG in solution, only reduced approximately 16% of nitrate during the first hour of the UV irradiation (Figure 2), and all nitrate was converted to nitrite, a more toxic end product than nitrate (Figure S4). These results indicate that the photo-oxidative catalyst is ineffective at removing nitrate, mainly due to a deficiency in releasing electrons. In contrast, the photo-reductive TiO<sub>2</sub> removed more than 95% of nitrate at the end of the photochemical reaction, six times faster than the traditional photo-oxidative TiO<sub>2</sub>. The incorporation of surface-bound DEG ligands to the TiO<sub>2</sub> nanocrystal surfaces hindered the electron-hole recombination. Thus, photo-reductive TiO<sub>2</sub> kinetics improves compared to the standard photo-oxidative catalyst.

The UV control, in which nitrate was in contact with the synthesized nanoparticles in the absence of UV irradiation, demonstrated an insignificant extent of nitrate removal over the course of the experiment, likely due to mild effects of direct photolysis. The catalyst control, in which nitrate was irradiated by UV light but without the synthesized catalyst showed that approximately 23% of nitrate was removed via direct photolysis (Figure 2). Nitrite was produced as the major end product during nitrate direct photolysis (Figure S5). Photolysis of nitrate generates highly oxidative hydroxyl radical, and undergoes a series of photochemical pathways generating toxic nitrite as a byproduct.<sup>39,40</sup>

In the presence of DEG-bonded photo-reductive  $\text{TiO}_2$  catalyst under UV irradiation, nitrate was reduced at the fastest kinetics, and ammonium ion was generated as the main final product at the end of the reaction. Nitrite was initially produced but readily declined to a negligible level at the end of the UV exposure (Figure 3). Dissolved inorganic nitrogen, defined as the summation of nitrate, nitrite and ammonium nitrogen, was reduced by approximately 25% by the end of the reaction. Total nitrogen data suggested that the loss of dissolved inorganic nitrogen was converted to both nitrogenous gasses and organic nitrogen species (Figure S6).

### 3.3 Effects of $\text{TiO}_2$ synthesis temperature on ammonia selectivity and nitrate removal

The selectivity on ammonia production from nitrate removal in the photocatalytic system was further optimized by changing the  $\text{TiO}_2$  synthesis temperature during the crystallization process of the  $\text{TiO}_2$  nanocrystals. The selectivity of ammonium is defined as the ratio of the final ammonium concentration with respect to the extent of nitrate removal as follows:

$$\text{Selectivity of ammonium} = \frac{[\text{NH}_4^+]_{\text{final}}}{[\text{NO}_3^-]_{\text{ini}} - [\text{NO}_3^-]_{\text{final}}} \times 100\% \quad (1)$$

Where  $[\text{NH}_4^+]_{\text{final}}$  is the concentration of ammonium at the end of the reaction,  $[\text{NO}_3^-]_{\text{ini}}$  is the concentration of nitrate at the start of the reaction, and  $[\text{NO}_3^-]_{\text{final}}$  is the concentration of nitrate at the end of the reaction; all in units of mM. Results showed that the synthesis temperature greatly affected the ability of the  $\text{TiO}_2$  to selectively produce ammonium ion (Figure 4). In general, a higher synthesis temperature resulted in a higher selectivity of the ammonium ion production (Figure 4A). Specifically, the ammonium selectivity increased from 51% to 71%

when the TiO<sub>2</sub> synthesis temperature increased from 190°C to 230°C (Figure 4A). This suggests that a higher temperature yields a higher crystallinity in TiO<sub>2</sub> nanocrystals that favored ammonium ion formation pathway, consistent with the enhanced atomic mobility during the high-temperature growth.<sup>26,41,42</sup> TiO<sub>2</sub> synthesized at the highest experimental temperature of 230°C also exhibited the highest nitrate reduction kinetics (Figure 4B). The effect of synthesis temperature is limited by the boiling point of DEG. Meanwhile, TiO<sub>2</sub> synthesized at the highest temperature of 230°C exhibited the minimal transient formation of toxic nitrite (Figure 4C).

### 3.4 Environmental Implications

The DEG-bonded TiO<sub>2</sub> photocatalyst is effective at removing nitrate and converting it to the desirable end product of ammonium ion, with a minimal formation of nitrite. The comparison of nitrate reduction kinetics to the traditional photo-oxidative TiO<sub>2</sub> catalyst demonstrated the advantages of the new catalyst to existing nitrogen removal technologies. The TiO<sub>2</sub> catalyst synthesized at 230°C demonstrates the best performance in nitrate reduction kinetics and the highest selectivity in converting nitrate to ammonium ion, with a selectivity of approximately 70%. To further demonstrate the catalyst performance and selectivity in real waters, a synthetic nitrate-contaminated groundwater matrix was prepared. This test was aimed to evaluate the effects of various ionic constituents commonly present in nitrate-contaminated groundwater (Table S1). Treatment of the synthetic groundwater with photo-reductive TiO<sub>2</sub> showed that nitrate was fully removed and the selectivity of ammonium ion was comparable to that in a DI water matrix, while nitrite formation was minimal (Table S2). The results indicate that the nitrate reduction kinetics at this time frame was reduced only 4%, with a nitrate removal efficiency of

95%. Furthermore, the selectivity of ammonium ion was still generated at 60% selectivity with no nitrite formation at these conditions. This bench-scale experiment demonstrated the promising real-world application of the synthesized DEG-doped TiO<sub>2</sub> nanoparticles to effectively treat nitrate from contaminated water and selectively recover the nitrogen resources, via exposing nitrate contaminated wastewaters to polychromatic UV light. Ammonium ion generated from this photocatalytic process can be recovered via chemical precipitation as the final nitrogen fertilizer feedstock. For instance, struvite, NH<sub>4</sub>MgPO<sub>4</sub>, formation occurs spontaneously in systems containing ammonium, magnesium, and phosphate ions.<sup>43</sup> Prior studies indicate that parameters such as pH, temperature, and mixing speed affect the nucleation and growth rates of struvite crystallization.

#### **4. Conclusion**

The application of this novel, synthetic nanocrystal addresses the environmental implications of simultaneous nitrate removal and ammonium harvesting from nitrate-contaminated wastewater sources. The DEG-doped TiO<sub>2</sub> catalyst can effectively convert nitrate to ammonium ion as the end product in nitrate-contaminated water. The temperature during the low-gradient thermal hydrolysis of the TiO<sub>2</sub> synthesis process greatly affected the selectivity of ammonium ion. Higher synthesis temperatures enhanced the crystallinity of the catalyst and positively correlated with the selectivity. Results showed that the catalyst synthesized at 230°C generated the highest ammonium selectivity compared to catalysts synthesized at lower temperatures, up to 71% of nitrate conversion to ammonium. This synthetic non-harsh and non-toxic nanoparticle can be feasibly applied to nitrate contaminated wastewater sources, including groundwater and

agricultural runoff wastewaters. Further work will be conducted to optimize the ammonium ion generation kinetics and UV wavelengths. Additionally, a better mechanistic understanding on the nitrogen transformation pathways is warranted.

### **Acknowledgements**

The study was supported by the United States Department of Agriculture (USDA AFRI Award 2020-65210-30764). We are also thankful for assistance from Dr. Ji Feng for analysis of TEM results and insightful discussions and for Samantha Ying, Monica Hope, and David Lyons for assistance with total aqueous phase nitrogen acquisition.

### **Supporting Information Section**

Additional text and figures showing nitrogen speciation during photocatalytic denitrification are provided in the Supporting Information Section.



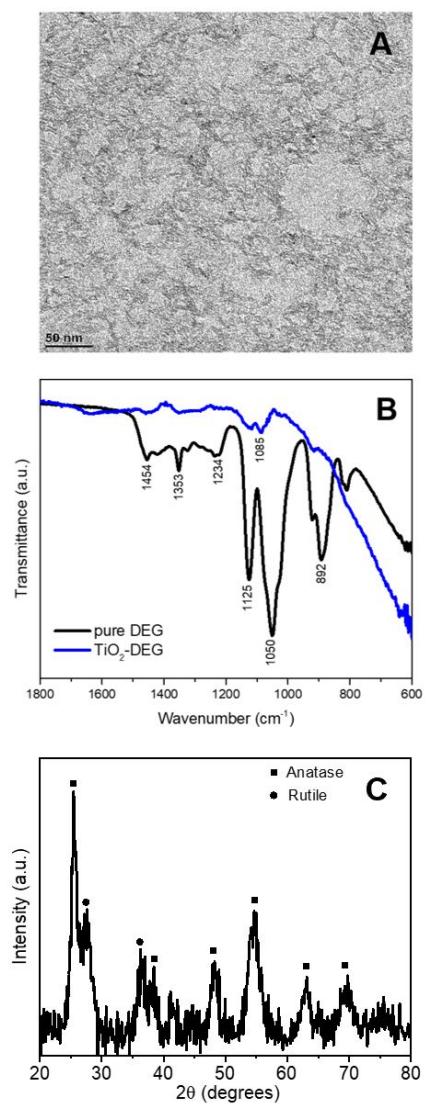


**Figure 1.** Characterization of synthesized photo-reductive DEG-doped TiO<sub>2</sub> catalyst. The catalyst was synthesized in diethylene glycol (DEG) at 230°C for 3 hours. (A) TEM image of TiO<sub>2</sub> nanocrystals; (B) FTIR spectra of TiO<sub>2</sub> nanocrystals and DEG; (C) XRD Pattern.

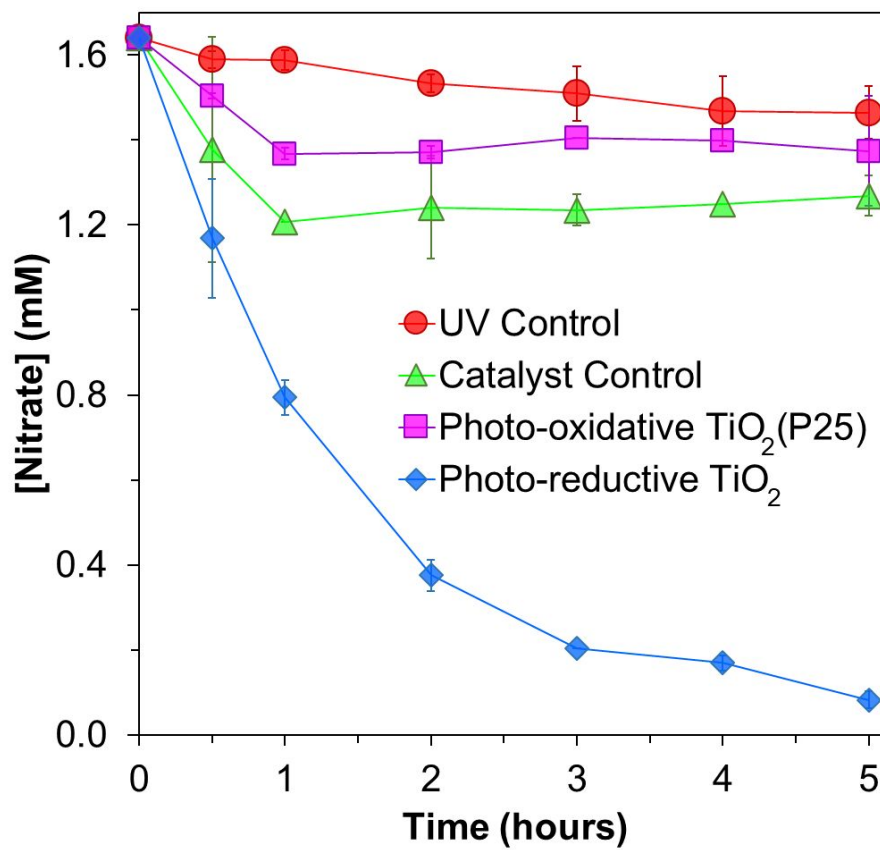


**Figure 2.** Reaction kinetics of nitrate reduction in different photochemical systems with controls.  $[\text{TiO}_2] = 50 \text{ mg/L}$ ,  $\text{pH} = 7$  irradiated under medium pressure UV light. UV control was conducted without UV irradiation and in the presence of photo-reductive  $\text{TiO}_2$ . Catalyst control was conducted with UV irradiation and in the absence of photo-reductive  $\text{TiO}_2$ . Photo-oxidative  $\text{TiO}_2$  experiment was conducted in the presence of commercial P25 in DEG solution. Photo-oxidative  $\text{TiO}_2$  experiment was conducted with the synthesized DEG-doped  $\text{TiO}_2$ .

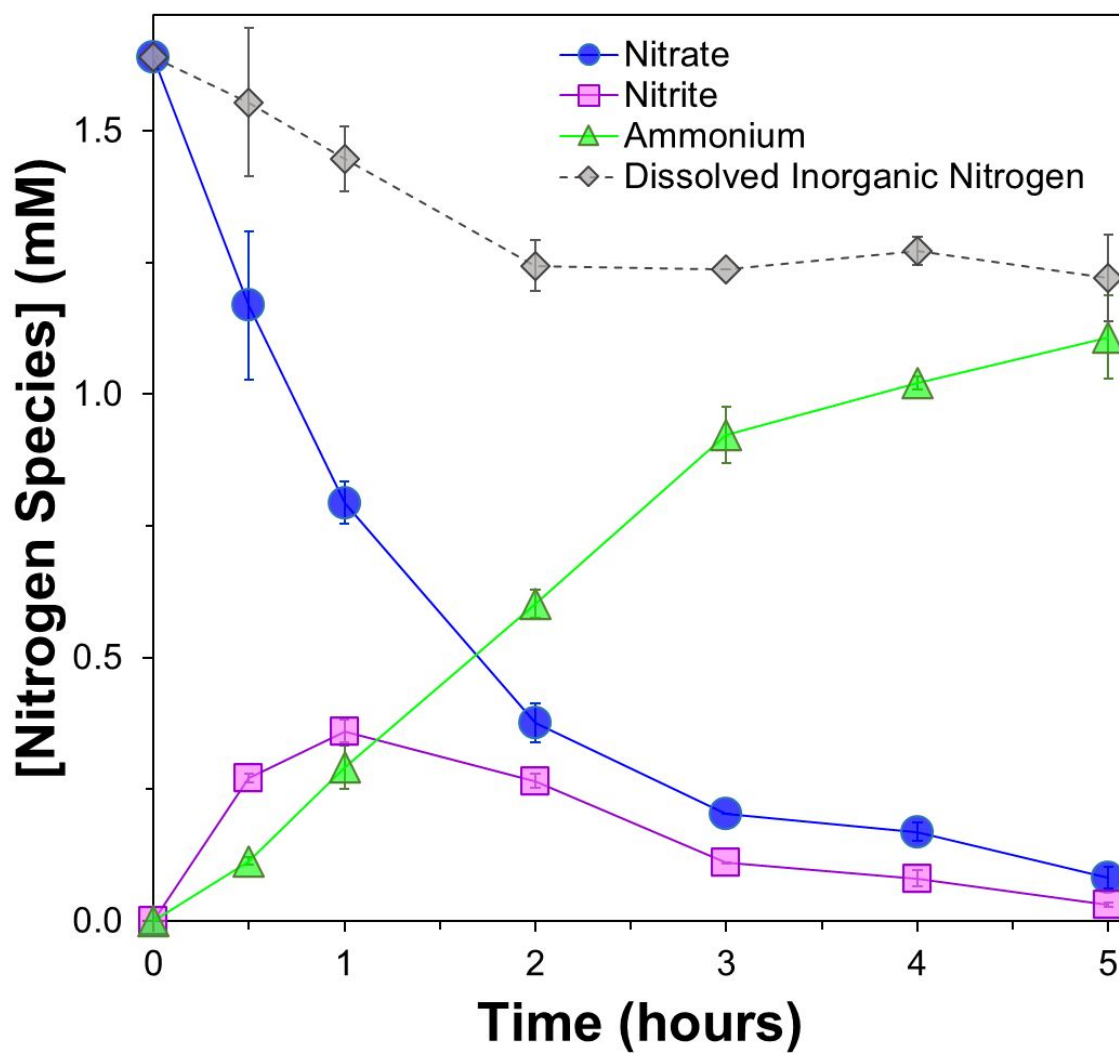


**Figure 3.** Nitrogen speciation profile for the reduction of nitrate in the presence of  $\text{TiO}_2$  catalyst synthesized at  $230^\circ\text{C}$ .  $[\text{Nitrate}] = 1.64 \text{ mM}$ ,  $[\text{TiO}_2] = 50 \text{ mg/L}$ ,  $\text{pH}=7$ . Dissolved inorganic nitrogen calculated as the sum of nitrate, nitrite, and ammonium.

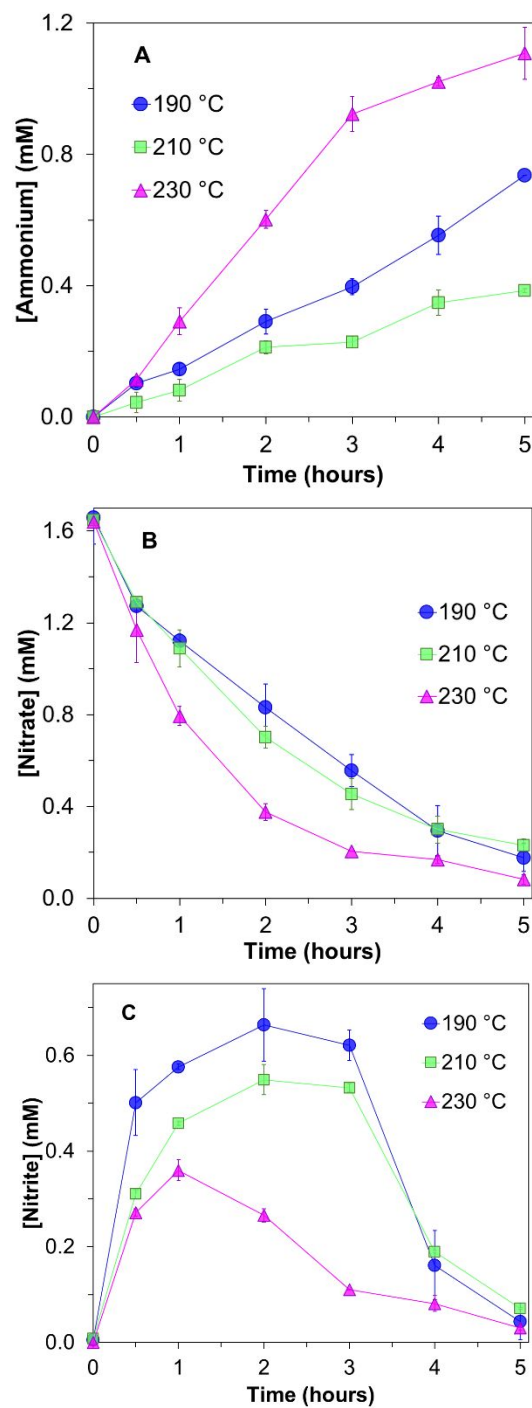


**Figure 4.** Effects of synthesis temperature on (A) ammonium formation, (B) nitrate reduction, and (C) nitrite generation and reduction. [Nitrate] = 1.64 mM, [TiO<sub>2</sub>] = 50 mg/L, pH=7.

## References

- (1) Taylor, P. G.; Townsend, A. R. Stoichiometric Control of Organic Carbon–Nitrate Relationships from Soils to the Sea. *Nature* **2010**, *464* (7292), 1178–1181. <https://doi.org/10.1038/nature08985>.
- (2) Galloway, J. N.; Townsend, A. R.; Erismann, J. W.; Bekunda, M.; Cai, Z.; Freney, J. R.; Martinelli, L. A.; Seitzinger, S. P.; Sutton, M. A. Transformation of the Nitrogen Cycle: Recent Trends, Questions, and Potential Solutions. *Science* **2008**, *320* (5878), 889–892. <https://doi.org/10.1126/science.1136674>.
- (3) Smil, V. Nitrogen in Crop Production: An Account of Global Flows. *Global Biogeochem. Cycles* **1999**, *13* (2), 647–662. <https://doi.org/10.1029/1999GB900015>.
- (4) Doudrick, K.; Yang, T.; Hristovski, K.; Westerhoff, P. Photocatalytic Nitrate Reduction in Water: Managing the Hole Scavenger and Reaction by-Product Selectivity. *Applied Catalysis B: Environmental* **2013**, *136–137*, 40–47. <https://doi.org/10.1016/j.apcatb.2013.01.042>.
- (5) Manassaram Deana M.; Backer Lorraine C.; Moll Deborah M. A Review of Nitrates in Drinking Water: Maternal Exposure and Adverse Reproductive and Developmental Outcomes. *Environmental Health Perspectives* **2006**, *114* (3), 320–327. <https://doi.org/10.1289/ehp.8407>.
- (6) Spalding, R. F.; Exner, M. E. Occurrence of Nitrate in Groundwater—A Review. *Journal of Environmental Quality* **1993**, *22* (3), 392–402. <https://doi.org/10.2134/jeq1993.00472425002200030002x>.
- (7) Yamauchi, M.; Abe, R.; Tsukuda, T.; Kato, K.; Takata, M. Highly Selective Ammonia Synthesis from Nitrate with Photocatalytically Generated Hydrogen on CuPd/TiO<sub>2</sub>. *J Am Chem Soc* **2011**, *133* (5), 1150–1152. <https://doi.org/10.1021/ja106285p>.
- (8) Reeves, T. G. Nitrogen Removal: A Literature Review. *Journal (Water Pollution Control Federation)* **1972**, *44* (10), 1895–1908.
- (9) Khin, T.; Annachhatre, A. P. Novel Microbial Nitrogen Removal Processes. *Biotechnology Advances* **2004**, *22* (7), 519–532. <https://doi.org/10.1016/j.biotechadv.2004.04.003>.
- (10) van der Hoek, J. P.; van der Ven, P. J. M.; Klapwijk, A. Combined Ion Exchange/Biological Denitrification for Nitrate Removal from Ground Water under Different Process Conditions. *Water Research* **1988**, *22* (6), 679–684. [https://doi.org/10.1016/0043-1354\(88\)90178-9](https://doi.org/10.1016/0043-1354(88)90178-9).

- (11) Robertson, L. A.; Kuenen, J. G. Combined Heterotrophic Nitrification and Aerobic Denitrification in Thiosphaera Pantotropha and Other Bacteria. *Antonie van Leeuwenhoek* **1990**, *57* (3), 139–152. <https://doi.org/10.1007/BF00403948>.
- (12) Wang, Y.; Wang, C.; Li, M.; Yu, Y.; Zhang, B. Nitrate Electroreduction: Mechanism Insight, in Situ Characterization, Performance Evaluation, and Challenges. *Chem. Soc. Rev.* **2021**, *50* (12), 6720–6733. <https://doi.org/10.1039/D1CS00116G>.
- (13) Yang, T.; Doudrick, K.; Westerhoff, P. Photocatalytic Reduction of Nitrate Using Titanium Dioxide for Regeneration of Ion Exchange Brine. *Water Research* **2013**, *47* (3), 1299–1307. <https://doi.org/10.1016/j.watres.2012.11.047>.
- (14) Zhang, X.; Wang, Y.; Liu, C.; Yu, Y.; Lu, S.; Zhang, B. Recent Advances in Non-Noble Metal Electrocatalysts for Nitrate Reduction. *Chemical Engineering Journal* **2021**, *403*, 126269. <https://doi.org/10.1016/j.cej.2020.126269>.
- (15) Ni, B.-J.; Pan, Y.; Guo, J.; Viridis, B.; Hu, S.; Chen, X.; Yuan, Z. CHAPTER 16: Denitrification Processes for Wastewater Treatment. In *Metalloenzymes in Denitrification*; 2016; pp 368–418. <https://doi.org/10.1039/9781782623762-00368>.
- (16) Chen, F.-Y.; Wu, Z.-Y.; Gupta, S.; Rivera, D. J.; Lambeets, S. V.; Pecaut, S.; Kim, J. Y. T.; Zhu, P.; Finprock, Y. Z.; Meira, D. M.; King, G.; Gao, G.; Xu, W.; Cullen, D. A.; Zhou, H.; Han, Y.; Perea, D. E.; Muhich, C. L.; Wang, H. Efficient Conversion of Low-Concentration Nitrate Sources into Ammonia on a Ru-Dispersed Cu Nanowire Electrocatalyst. *Nat. Nanotechnol.* **2022**, 1–9. <https://doi.org/10.1038/s41565-022-01121-4>.
- (17) Chang, H.; Lu, M.; Zhu, Y.; Zhang, Z.; Zhou, Z.; Liang, Y.; Vidic, R. D. Consideration of Potential Technologies for Ammonia Removal and Recovery from Produced Water. *Environ. Sci. Technol.* **2022**, *56* (6), 3305–3308. <https://doi.org/10.1021/acs.est.1c08517>.
- (18) Hirakawa, H.; Hashimoto, M.; Shiraishi, Y.; Hirai, T. Photocatalytic Conversion of Nitrogen to Ammonia with Water on Surface Oxygen Vacancies of Titanium Dioxide. *J. Am. Chem. Soc.* **2017**, *139* (31), 10929–10936. <https://doi.org/10.1021/jacs.7b06634>.
- (19) Lu, X.; Song, H.; Cai, J.; Lu, S. Recent Development of Electrochemical Nitrate Reduction to Ammonia: A Mini Review. *Electrochemistry Communications* **2021**, *129*, 107094. <https://doi.org/10.1016/j.elecom.2021.107094>.
- (20) Wang, J.; Feng, J.; Soyol-Erdene, T.-O.; Wei, Z.; Tang, W. Electrodeposited NiCoP on Nickel Foam as a Self-Supported Cathode for Highly Selective Electrochemical Reduction of Nitrate to Ammonia. *Separation and Purification Technology* **2023**, *320*, 124155. <https://doi.org/10.1016/j.seppur.2023.124155>.

- (21) Li, X.; Xing, W.; Hu, T.; Luo, K.; Wang, J.; Tang, W. Recent Advances in Transition-Metal Phosphide Electrocatalysts: Synthetic Approach, Improvement Strategies and Environmental Applications. *Coordination Chemistry Reviews* **2022**, *473*, 214811. <https://doi.org/10.1016/j.ccr.2022.214811>.
- (22) Sá, J.; Agüera, C. A.; Gross, S.; Anderson, J. A. Photocatalytic Nitrate Reduction over Metal Modified TiO<sub>2</sub>. *Applied Catalysis B: Environmental* **2009**, *85* (3), 192–200. <https://doi.org/10.1016/j.apcatb.2008.07.014>.
- (23) Wang, W.; Ye, M.; He, L.; Yin, Y. Nanocrystalline TiO<sub>2</sub>-Catalyzed Photoreversible Color Switching. *Nano Lett.* **2014**, *14* (3), 1681–1686. <https://doi.org/10.1021/nl500378k>.
- (24) Dal Santo, V.; Naldoni, A. *Titanium Dioxide Photocatalysis*; 2019.
- (25) Gopinath, K. P.; Madhav, N. V.; Krishnan, A.; Malolan, R.; Rangarajan, G. Present Applications of Titanium Dioxide for the Photocatalytic Removal of Pollutants from Water: A Review. *Journal of Environmental Management* **2020**, *270*, 110906. <https://doi.org/10.1016/j.jenvman.2020.110906>.
- (26) Liu, H.; Bong Joo, J.; Dahl, M.; Fu, L.; Zeng, Z.; Yin, Y. Crystallinity Control of TiO<sub>2</sub> Hollow Shells through Resin-Protected Calcination for Enhanced Photocatalytic Activity. *Energy & Environmental Science* **2015**, *8* (1), 286–296. <https://doi.org/10.1039/C4EE02618G>.
- (27) Kohtani, S.; Kawashima, A.; Miyabe, H. Reactivity of Trapped and Accumulated Electrons in Titanium Dioxide Photocatalysis. *Catalysts* **2017**, *7* (10), 303. <https://doi.org/10.3390/catal7100303>.
- (28) Sohn, Y.; Huang, W.; Taghipour, F. Recent Progress and Perspectives in the Photocatalytic CO<sub>2</sub> Reduction of Ti-Oxide-Based Nanomaterials. *Applied Surface Science* **2017**, *396*, 1696–1711. <https://doi.org/10.1016/j.apsusc.2016.11.240>.
- (29) Aleisa, R.; Feng, J.; Ye, Z.; Yin, Y. Rapid High-Contrast Photoreversible Coloration of Surface-Functionalized N-Doped TiO<sub>2</sub> Nanocrystals for Rewritable Light-Printing. *Angewandte Chemie n/a* (n/a), e202203700. <https://doi.org/10.1002/ange.202203700>.
- (30) Liu, Y.; Wang, M.; Li, D.; Fang, F.; Huang, W. Engineering Self-Doped Surface Defects of Anatase TiO<sub>2</sub> Nanosheets for Enhanced Photocatalytic Efficiency. *Applied Surface Science* **2021**, *540*, 148330. <https://doi.org/10.1016/j.apsusc.2020.148330>.
- (31) Chen, G.; Feng, J.; Wang, W.; Yin, Y.; Liu, H. Photocatalytic Removal of Hexavalent Chromium by Newly Designed and Highly Reductive TiO<sub>2</sub> Nanocrystals. *Water Research* **2017**, *108*, 383–390. <https://doi.org/10.1016/j.watres.2016.11.013>.

- (32) Zhao, Z.; Sun, Y.; Dong, F. Graphitic Carbon Nitride Based Nanocomposites: A Review. *Nanoscale* **2014**, *7* (1), 15–37. <https://doi.org/10.1039/C4NR03008G>.
- (33) Varapragasam, S. J. P.; Andriolo, J. M.; Skinner, J. L.; Grumstrup, E. M. Photocatalytic Reduction of Aqueous Nitrate with Hybrid Ag/g-C<sub>3</sub>N<sub>4</sub> under Ultraviolet and Visible Light. *ACS Omega* **2021**, *6* (50), 34850–34856. <https://doi.org/10.1021/acsomega.1c05523>.
- (34) Chen, S.; Liu, X.; Xiong, J.; Mi, L.; Song, X.-Z.; Li, Y. Defect and Interface Engineering in Metal Sulfide Catalysts for the Electrocatalytic Nitrogen Reduction Reaction: A Review. *Journal of Materials Chemistry A* **2022**, *10* (13), 6927–6949. <https://doi.org/10.1039/D2TA00070A>.
- (35) Richards, D.; D. Young, S.; R. Goldsmith, B.; Singh, N. Electrocatalytic Nitrate Reduction on Rhodium Sulfide Compared to Pt and Rh in the Presence of Chloride. *Catalysis Science & Technology* **2021**, *11* (22), 7331–7346. <https://doi.org/10.1039/D1CY01369F>.
- (36) Morozan, A.; Jaouen, F. Metal Organic Frameworks for Electrochemical Applications. *Energy & Environmental Science* **2012**, *5* (11), 9269–9290. <https://doi.org/10.1039/C2EE22989G>.
- (37) Baird, R.; Eaton, A.; Rice, E. *Standard Methods for the Examination of Water and Wastewater*, 23rd ed.; American Public Health Association, 2017.
- (38) Feng, J.; Yang, F.; Ye, Y.; Wang, W.; Yao, X.; Fan, Q.; Liu, L.; Aleisa, R. M.; Guo, J.; Yin, Y. Surface-Bound Sacrificial Electron Donors in Promoting Photocatalytic Reduction on Titania Nanocrystals. *Nanoscale* **2019**, *11* (41), 19512–19519. <https://doi.org/10.1039/C9NR05453G>.
- (39) Mack, J.; Bolton, J. R. Photochemistry of Nitrite and Nitrate in Aqueous Solution: A Review. *Journal of Photochemistry and Photobiology A: Chemistry* **1999**, *128* (1), 1–13. [https://doi.org/10.1016/S1010-6030\(99\)00155-0](https://doi.org/10.1016/S1010-6030(99)00155-0).
- (40) Chen, G.; Hanukovich, S.; Chebeir, M.; Christopher, P.; Liu, H. Nitrate Removal via a Formate Radical-Induced Photochemical Process. *Environ. Sci. Technol.* **2019**, *53* (1), 316–324. <https://doi.org/10.1021/acs.est.8b04683>.
- (41) Bong Joo, J.; Dahl, M.; Li, N.; Zaera, F.; Yin, Y. Tailored Synthesis of Mesoporous TiO<sub>2</sub> Hollow Nanostructures for Catalytic Applications. *Energy & Environmental Science* **2013**, *6* (7), 2082–2092. <https://doi.org/10.1039/C3EE41155A>.
- (42) Joo, J. B.; Zhang, Q.; Lee, I.; Dahl, M.; Zaera, F.; Yin, Y. Mesoporous Anatase Titania Hollow Nanostructures Through Silica-Protected Calcination. *Advanced Functional Materials* **2012**, *22* (1), 166–174. <https://doi.org/10.1002/adfm.201101927>.



- (43) Doyle, J. D.; Parsons, S. A. Struvite Formation, Control and Recovery. *Water Research* **2002**, *36* (16), 3925–3940. [https://doi.org/10.1016/S0043-1354\(02\)00126-4](https://doi.org/10.1016/S0043-1354(02)00126-4).